

Design, Synthesis, and Biological Activity of a Family of Novel Ceramide Analogues in Chemoresistant Breast Cancer Cells

James W. Antoon,^{†,§} Jiawang Liu,^{‡,§} Matthew M. Gestaut,[†] Matthew E. Burow,[†] Barbara S. Beckman,[†] and Maryam Foroozesh^{*,‡}

[†]Department of Pharmacology and Department of Medicine, Tulane University School of Medicine, 1430 Tulane Avenue, New Orleans, Louisiana 70112, and [‡]Department of Chemistry, Xavier University of Louisiana, 1 Drexel Drive, New Orleans, Louisiana 70125. [§]These authors contributed equally to this work.

Received May 11, 2009

Resistance to chemotherapy and endocrine therapy is a major cause of breast cancer treatment failure. We have synthesized six novel analogues using C8-ceramide as the lead analogue and studied their effect on hormone therapy resistant (MDA-MB-231) and chemoresistant (MCF-7TN-R) breast cancer cells. Pharmacologic intervention using these ceramide analogues inhibited clonogenic survival and induced apoptosis, with one analogue being more effective than C8-ceramide. Our results show ceramide-based therapy has therapeutic potential in treating drug resistant breast cancer.

Introduction

Breast cancer remains the predominant form of carcinoma affecting American women today, and resistance to chemotherapy and endocrine therapy is a major cause of treatment failure. Recent research suggests that pathogenic alterations in endogenous ceramide levels contribute to breast cancer chemoresistance.^{1–5} Targeting the bioactive sphingolipid ceramide is a promising approach because of its regulation of cellular apoptosis and survival. Several chemotherapeutic agents, including paclitaxel and doxorubicin, induce apoptosis through the induction of ceramide signaling as a mechanism of action.^{4,6} In fact, decreased synthesis and increased metabolism of ceramide have been shown to be important components of chemoresistance in human breast cancer.^{7–9}

Our laboratory previously showed that ceramide analogues, particularly 4,6-dieneceramide, have therapeutic potential in the treatment of chemosensitive and -resistant breast cancer.¹⁰ Here, we used C8-ceramide as the lead analogue for the design and synthesis of six novel ceramides analogues (Figure 1). In these analogues, we have incorporated a new amide functional group in the sphingosine backbone, replacing the original enol functional group (the C3 OH and the C4–C5 double bond of C8-Cer). This enol double bond is believed to be important in ceramide's biological activity. The presence of this new additional amide functional group is expected to change the polarity while testing the importance of the presence of C3 OH and C4–C5 double bond for optimum ceramide activity. The carbon chain length in the backbone was kept approximately the same as the known ceramides to maintain optimum lipid solubility and facility of passage through membranes. Other structural variations of our analogues include the presence and absence of the original amide carbonyl group and different sizes and shapes of the substituents on the original nitrogen.

These analogues were tested for their effect on breast cancer clonogenic survival and proapoptotic activity in the chemosensitive MCF-7, endocrine-resistant MDA-MB-231, and chemoresistant MCF-7TN-R breast cancer cell lines. The last two of these cell lines represent highly aggressive, metastatic, and drug resistant forms of human breast cancer. The MDA-MB-231 cell line is triple-negative (ER- α /PR/HER2 negative) and resistant to hormone and endocrine therapies. The MCF-7TN-R cell line was derived from MCF-7 cells grown in increasing concentrations of tumor necrosis factor until resistance was established.¹¹ These cells exhibit increased resistance to several chemotherapeutic agents including etoposide, paclitaxel, and doxorubicin. In all cell lines tested, we found that **3** was the most effective analogue and was more efficacious than ceramide in inducing apoptosis and preventing survival of chemoresistant breast cancer cells.

Experimental Section

General. All the chemicals were purchased from Sigma Chemical Co. All coupling and deprotection reactions were carried out under anhydrous conditions. The purities of the intermediates and the products were confirmed by thin layer chromatography (Whatman 250 μ m layer, UV₂₅₄, flexible plates for TLC and silica gel IB2-F). Chromatography was performed on HPTLC silica gel 60 F₂₅₄. ¹H NMR spectra were recorded on a Varian EM 360A spectrometer, and ¹³C NMR spectra were recorded on Varian 300 MHz spectrometer. Mass spectral data were determined by Micromass Quattro Micro API and Agilent 6890 GC with 5973 MS.

(S)-tert-Butyl 3-hydroxy-1-oxo-1-(tetradecylamino)propan-2-ylcarbamate Intermediate. An amount of 1.32 g (9.76 mmol) of 1-hydroxybenzotriazole hydrate (HOBt) was added at 0 °C to a solution of 2.00 g (9.76 mmol) of *N*-Boc-L-serine in 60 mL of anhydrous tetrahydrofuran (THF). The pH of the solution was adjusted to 8–9 with 4-methylmorpholine. After the mixture was stirred for 5 min, 2.21 g (10.74 mmol) of *N,N'*-dicyclohexylcarbodiimide (DCC) was added. A solution of 2.08 g (9.76 mmol) of tetradecylamine in 3 mL of anhydrous THF was added to a

*To whom correspondence should be addressed. Phone: 504-520-5078. Fax: 504-520-7942. E-mail: mforooze@xula.edu.

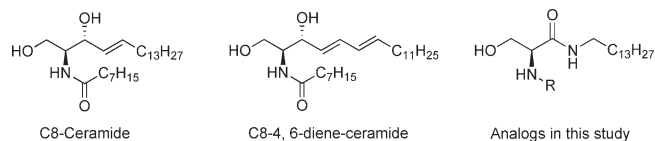


Figure 1. Structures of C8-ceramide, C8-4,6-dieneceramide, and target analogues studied.

solution of *N*-Boc-L-serine, and the mixture was stirred at 0 °C for 2 h and at room temperature overnight. On evaporation the residue was dissolved in 60 mL of ethyl acetate. The solution was washed successively with saturated sodium bicarbonate, 5% potassium bisulfate, and saturated sodium chloride, and the organic phase was separated and dried over anhydrous magnesium sulfate for 2 h. After filtration and evaporation under reduced pressure 3.57 g (91.5%) of (*S*)-*tert*-butyl 3-hydroxy-1-oxo-1-(tetradecylamino)propan-2-ylcarbamate was obtained as a powder. ¹H NMR (DMSO-*d*₆, 60 MHz) δ/ppm = 7.708 (t, *J* = 5.1 Hz, 1H), 6.507 (d, *J* = 7.9 Hz, 1H), 4.765 (t, *J* = 5.1 Hz, 1H), 3.881 (m, 1H), 3.525 (m, 2H), 3.076 (m, 2H), 1.401 (s, 9H), 1.589–0.740 (m, 36H). ¹³C NMR (DMSO-*d*₆, 75 MHz) δ/ppm = 170.725, 155.784, 78.683, 62.558, 57.548, 39.161, 31.994, 29.732, 29.504, 29.413, 28.790, 26.953, 22.778, 14.548.

(*S*)-2-Amino-3-hydroxy-*N*-tetradecylpropanamide Intermediate. At 0 °C, to a solution of 1.00 g (2.50 mmol) of (*S*)-*tert*-butyl 3-hydroxy-1-oxo-1-(tetradecylamino)propan-2-ylcarbamate in 20 mL of dichloromethane (DCM), 3.0 mL of trifluoroacetic acid was added. After the mixture was stirred for 4 h, the solvent was removed under vacuum pressure, and the residue was crystallized in diethyl ether and petroleum ether to give 0.68 g (65.7%) of (*S*)-2-amino-3-hydroxy-*N*-tetradecylpropanamide as a powder. ¹H NMR (DMSO-*d*₆, 60 MHz) δ/ppm = 8.358 (t, *J* = 6.0 Hz, 1H), 8.112 (m, 3H), 4.583 (br, 1H), 3.715 (m, 3H), 3.093 (m, 2H), 1.531–0.677 (m, 27H). ¹³C NMR (DMSO-*d*₆, 75 MHz) δ/ppm = 167.141, 61.040, 55.042, 39.449, 31.979, 29.747, 29.701, 29.489, 29.398, 26.968, 22.763, 14.563.

Analogue 1: (*S*)-*N*-(3-Hydroxy-1-oxo-1-(tetradecylamino)propan-2-yl)cyclohexanecarboxamide. At 0 °C, to a solution of 0.16 g (1.20 mmol) of cyclohexanecarboxylic acid in anhydrous THF (20 mL) and DMF (5 mL), 0.16 g (1.20 mmol) of HOBt and 0.50 g (1.20 mmol) of (*S*)-2-amino-3-hydroxy-*N*-tetradecylpropanamide were added. After 5 min, 0.30 g (1.45 mmol) of DCC was added, and the pH of the solution was adjusted to 8–9 with 4-methylmorpholine. The mixture was stirred at 0 °C for 2 h and at room temperature overnight. On evaporation the residue was dissolved in 100 mL of ethyl acetate. The solution was washed successively with saturated sodium bicarbonate, 5% potassium bisulfate, and saturated sodium chloride, and the organic phase was separated and dried over anhydrous magnesium sulfate for 2 h. After filtration and evaporation under reduced pressure 0.40 g (81.3%) of (*S*)-*N*-(3-hydroxy-1-oxo-1-(tetradecylamino)propan-2-yl)cyclohexanecarboxamide was obtained as powder. ESI/MS (*m/e*) 411 [M + H]⁺. ¹H NMR (DMSO-*d*₆, 60 MHz) δ/ppm = 7.559 (m, 2H), 4.762 (t, *J* = 5.1 Hz, 1H), 4.195 (m, 1H), 3.495 (m, 3H), 3.020 (m, 2H), 1.912–0.711 (m, 37H). ¹³C NMR (DMSO-*d*₆, 75 MHz) δ/ppm = 175.841, 170.649, 62.452, 55.604, 44.368, 39.145, 34.029, 31.979, 29.884, 29.717, 29.458, 29.382, 26.938, 26.164, 26.012, 25.146, 22.778, 14.609. Anal. Calcd for C₂₄H₄₆N₂O₃: C, 70.20; H, 11.29; N, 6.82; O, 11.69. Found: C, 69.34; H, 11.25; N, 6.52; O, 12.42.

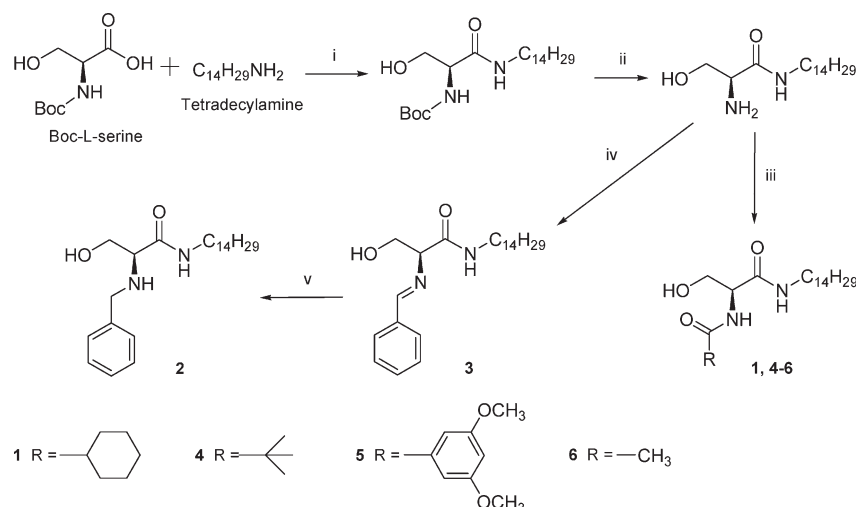
Analogue 2: (*S*)-2-(Benzylamino)-3-hydroxy-*N*-tetradecylpropanamide. To a solution of 0.20 g (0.52 mmol) of (*S*)-2-(benzylideneamino)-3-hydroxy-*N*-tetradecylpropanamide in 10 mL of methanol, 32 mg (0.52 mmol) of sodium borohydride (NaBH₄) was added. The mixture was stirred at room temperature for 10 h before evaporation under vacuum. The residue was purified by thin layer chromatography to give 115 mg (57.5%) of (*S*)-2-(benzylamino)-3-hydroxy-*N*-tetradecylpropanamide as a colorless powder. ESI/MS (*m/e*) 391 [M + H]⁺. ¹H NMR (DMSO-*d*₆,

60 MHz) δ/ppm = 7.780 (t, *J* = 5.1 Hz, 1H), 7.304 (m, 5H), 4.726 (br, 1H), 3.790–2.869 (m, 7H), 1.566–0.706 (m, 27H). ¹³C NMR (DMSO-*d*₆, 75 MHz) δ/ppm = 172.425, 141.041, 128.788, 128.651, 127.361, 64.638, 63.150, 52.097, 38.902, 31.979, 29.853, 29.717, 29.413, 29.382, 27.014, 22.763, 14.609. Anal. Calcd for C₂₄H₄₂N₂O₂: C, 73.80; H, 10.84; N, 7.17; O, 8.19. Found: C, 71.64; H, 10.63; N, 6.75; O, 9.10.

Analogue 3: (*S*)-2-(Benzylideneamino)-3-hydroxy-*N*-tetradecylpropanamide. A mixture of 0.50 g (1.20 mmol) of (*S*)-2-amino-3-hydroxy-*N*-tetradecylpropanamide, 0.05 g (1.20 mmol) of NaOH, 0.13 g (1.20 mmol) of benzaldehyde, and 10 mL of methanol was stirred at room temperature for 8 h. The solvent was then evaporated under reduced pressure, and the residue was washed with cooled methanol to yield 0.32 g (68.7%) of (*S*)-2-(benzylideneamino)-3-hydroxy-*N*-tetradecylpropanamide as colorless powder. ESI/MS (*m/e*) 389 [M + H]⁺. ¹H NMR (DMSO-*d*₆, 60 MHz) δ/ppm = 8.281 (s, 1H), 7.818 (m, 3H), 7.515 (m, 3H), 4.795 (br, 1H), 3.768 (m, 3H), 3.103 (m, 2H), 1.584–0.702 (m, 27H). ¹³C NMR (DMSO-*d*₆, 75 MHz) δ/ppm = 170.497, 163.239, 136.532, 131.597, 129.198, 129.061, 76.254, 63.788, 39.039, 31.964, 29.808, 29.701, 29.382, 26.983, 22.763, 14.609. Anal. Calcd for C₂₄H₄₀N₂O₂: C, 74.18; H, 10.38; N, 7.21; O, 8.23. Found: C 72.83; H, 10.44; N, 7.14; O, 8.77.

Analogue 4: (*S*)-3-Hydroxy-2-pivalamido-*N*-tetradecylpropanamide. At 0 °C to a solution of 0.10 g (0.98 mmol) of trimethylacetic acid in anhydrous THF (60 mL), 0.13 g (0.96 mmol) of HOBt and 0.40 g (0.97 mmol) of (*S*)-2-amino-3-hydroxy-*N*-tetradecylpropanamide were added. After 5 min, 0.23 g (1.12 mmol) of DCC was added and the pH of the solution was adjusted to 8–9 with 4-methylmorpholine. The mixture was stirred at 0 °C for 2 h and at room temperature overnight. On evaporation the residue was dissolved in 100 mL of ethyl acetate. The solution was washed successively with saturated sodium bicarbonate, 5% potassium bisulfate, and saturated sodium chloride, and the organic phase was separated and dried over anhydrous magnesium sulfate for 2 h. After filtration and evaporation under reduced pressure 0.28 g (72.9%) of (*S*)-3-hydroxy-2-pivalamido-*N*-tetradecylpropanamide was obtained as a powder. ESI/MS (*m/e*) 385 [M + H]⁺. ¹H NMR (DMSO-*d*₆, 90 MHz) δ/ppm = 7.642 (t, *J* = 5.1 Hz, 1H), 7.088 (d, *J* = 7.9 Hz, 1H), 4.818 (t, *J* = 5.1 Hz, 1H), 4.198 (m, 1H), 3.552 (m, 2H), 3.037 (m, 2H), 1.124 (s, 9H), 1.572–0.728 (m, 36H). ¹³C NMR (DMSO-*d*₆, 75 MHz) δ/ppm = 177.861, 170.558, 62.406, 55.908, 39.161, 31.979, 29.732, 29.701, 29.443, 29.398, 27.910, 26.938, 22.778, 14.609. Anal. Calcd for C₂₂H₄₄N₂O₃: C, 68.70; H, 11.53; N, 7.28; O, 12.48. Found: C 68.25; H, 11.51; N, 7.10; O, 13.09.

Analogue 5: (*S*)-*N*-(3-Hydroxy-1-oxo-1-(tetradecylamino)propan-2-yl)-3,5-dimethoxybenzamide. At 0 °C to a solution of 0.18 g (1.0 mmol) of 3,5-dimethoxybenzoic acid in anhydrous THF (40 mL), 0.14 g (1.0 mmol) of HOBt and 0.30 g (1.0 mmol) of (*S*)-2-amino-3-hydroxy-*N*-tetradecylpropanamide were added. Then 0.23 g (1.1 mmol) of DCC was added, and the pH of the solution was adjusted to 8 with 4-methylmorpholine. The mixture was stirred at 0 °C for 2 h and at room temperature overnight. On evaporation the residue was dissolved in 100 mL of ethyl acetate. The solution was washed successively with saturated sodium bicarbonate, 5% potassium bisulfate, and saturated sodium chloride, and the organic phase was separated and dried over anhydrous magnesium sulfate for 2 h. After filtration and evaporation under reduced pressure, 0.38 g (82.0%) of (*S*)-*N*-(3-hydroxy-1-oxo-1-(tetradecylamino)propan-2-yl)-3,5-dimethoxybenzamide was obtained as a powder. GC/MS with BSTFA/TMCS (*m/e*) 518 [M + TMS – H₂O]⁺, 662 [M + 3TMS – H₂O]⁺. ¹H NMR (DMSO-*d*₆, 60 MHz) δ/ppm = 8.186 (d, *J* = 7.9 Hz, 1H), 7.830 (t, *J* = 5.1 Hz, 1H), 7.054 (d, *J* = 2.4 Hz, 2H), 6.700 (t, *J* = 2.4 Hz, 1H), 4.874 (t, *J* = 5.1 Hz, 1H), 4.413 (m, 1H), 3.788 (s, 6H), 3.674 (m, 2H), 3.054 (m, 2H), 1.708–0.705 (m, 27H). ¹³C NMR (DMSO-*d*₆, 75 MHz) δ/ppm = 170.345, 166.580, 160.946, 137.017, 106.150, 103.857, 62.361, 56.971, 56.120, 39.252, 31.979, 29.747, 29.701, 29.443, 29.398, 26.968, 22.778, 14.609. Anal.

Scheme 1. Synthesis Scheme for the Ceramide Analogues^a

^a(i) DCC/HOBT in THF 0 °C; (ii) TFA/CH₂Cl₂ (0 °C), NaCO₃/ethyl acetate; (iii) DCC/HOBT in THF 0 °C and different acids; (iv) NaOH/benzaldehyde in methanol; v) NaBH₃CN/methanol.

Calcd for C₂₆H₄₄N₂O₅: C, 67.21; H, 9.54; N, 6.03; O, 17.22. Found: C 65.08; H, 9.59; N, 6.05; O, 17.23.

Analogue 6: (S)-2-Acetamido-3-hydroxy-N-tetradecylpropanamide. At 0 °C to a solution of 0.026 mL (0.48 mmol) of acetic acid in anhydrous THF (50 mL), 32 mg (0.24 mmol) of HOBT and 0.10 g (0.24 mmol) of (S)-2-amino-3-hydroxy-N-tetradecylpropanamide were added. Then 53 mg (0.26 mmol) of DCC in 5 mL of THF was added, and the pH was adjusted to 7–8 with 4-methylmorpholine. The mixture was stirred at 0 °C for 2 h and at room temperature overnight. On evaporation the residue was dissolved in 80 mL of ethyl acetate. The solution was washed successively with saturated sodium bicarbonate, 5% potassium bisulfate, and saturated sodium chloride, and the organic phase was separated and dried over anhydrous magnesium sulfate for 2 h. After filtration and evaporation under reduced pressure crude product was obtained and recrystallized using ethyl acetate to obtain 0.06 g (73.0%) of (S)-2-acetamido-3-hydroxy-N-tetradecylpropanamide as a powder. GC/MS with BSTFA/TMCS (*m/e*) 414 [M + 1TMS]⁺, 468 [M + 2TMS - H₂O]⁺. ¹H NMR (DMSO-*d*₆, 60 MHz) δ/ppm = 7.730 (m, 2H), 4.775 (t, *J* = 5.1 Hz, 1H), 4.155 (m, 1H), 3.495 (m, 2H), 3.020 (m, 2H), 1.846 (s, 3H), 1.740–0.632 (m, 27H). ¹³C NMR (DMSO-*d*₆, 75 MHz) δ/ppm = 168.538, 61.617, 56.849, 39.297, 31.964, 29.717, 29.686, 29.580, 29.382, 26.923, 22.763, 14.609. Anal. Calcd for C₁₉H₃₈N₂O₃: C, 66.63; H, 11.18; N, 8.18; O, 14.01. Found: C 66.75; H, 10.39; N, 7.56; O, 13.46.

Results

Synthesis of Analogues 1–6. The synthetic route of analogues 1–6 is described in Scheme 1. Boc-protecting L-serine was coupled with tetradecylamine, giving (S)-*tert*-butyl-3-hydroxy-1-oxo-1-(tetradecylamino)propan-2-ylcarbamate in 91.5% yield. After removal of the *tert*-butoxycarbonyl (Boc) group with trifluoroacetic acid in dichloromethane, the common intermediate (S)-2-amino-3-hydroxy-N-tetradecylpropanamide was formed in 65.7% yield. Analogues 1, 4, 5, and 6 were produced through the coupling of (S)-2-amino-3-hydroxy-N-tetradecylpropanamide with cyclohexanecarboxylic acid (in 81.3% yield), pivalic acid (in 72.9% yield), 3,5-dimethoxybenzoic acid (in 82.0% yield), and acetic acid (in 73.0%), respectively. In the presence of sodium hydroxide, condensation with benzaldehyde in methanol provided 3 in 68.7% yield, which was reduced by NaBH₃CN to give 2 in 57.5% yield. These results show that all of these reactions

Table 1. IC₅₀ of Ceramide Analogues (μM)^a

compd	MCF-7	MDA-MB-231	MCF-7-TNR
DH-Cer	31.7	41.4	49.6
C8-Cer	4.2	3.0	8.6
Analog 1	7.2	11.5	23.5
Analog 2	5.0	10.5	15.2
Analog 3	4.7	2.4	7.7
Analog 4	6.7	6.1	11.1
Analog 5	11.2	6.6	15.0
Analog 6	44.7	75.1	52.7

^aThe IC₅₀ values were calculated from experiments shown in Figure 1, Supporting Information, using the formulas described in the Materials

occurred in mild conditions, and ceramide analogues were produced with acceptable yields.

Analogue 3 Displays the Greatest Antisurvival Effect in MDA-MB-231 and MCF-7TN-R Cells. The six ceramide analogues were compared for their inhibitory effect on breast cancer clonogenic survival. Cells were treated with varying concentrations of analogue, ranging from 0.1 to 20 μM for 10 days. Cell colonies were then fixed, stained, and recorded as percent vehicle control. The IC₅₀ values for the analogues are listed in Table 1. All analogues displayed antisurvival properties in drug-resistant and drug-sensitive breast cancers.

All six analogues showed biological activity in the MCF-7 cell line. Analogs 2 and 3, both missing the original amide carbonyl group, had the greatest efficacy in MCF-7 cells, with IC₅₀ of 5.0 μM (*p* < 0.01) and 4.7 μM (*p* < 0.001), respectively. Interestingly, these analogues also showed activity in endocrine-resistant MDA-MB-231 and chemoresistant MCF-7TN-R cells. Analogue 3 was the most potent antisurvival agent and more effective than C8-ceramide in treating drug-resistant breast cancer, with IC₅₀ of 2.4 μM in MDA-MB-231 cells and 7.7 μM in MCF-7TN-R cells, with *p* of 0.037 and 0.019, respectively. Analogue 6 was the least effective in all of the cell lines tested.

Since 3 showed the greatest efficacy compared to the other newly synthesized analogues, we tested the ability of this drug to induce apoptosis in MCF-7 cells. Using a cell death detection ELISA (Roche), we measured the amount of apoptosis with IC₅₀ treatments of 3 and C8-ceramide. As seen in Figure 2, 3 caused a 5.4-fold induction (*p* = 0.034) in

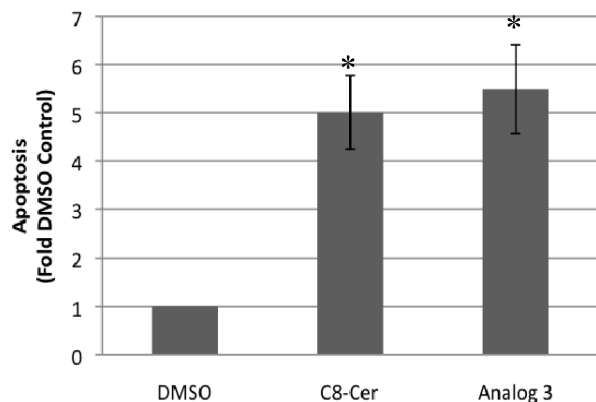


Figure 2. Effect of **3** on breast cancer apoptosis. MCF-7 cells were treated with double IC_{50} concentrations of ceramide ($8.3 \mu\text{M}$) and **3** ($9.4 \mu\text{M}$) for 24 h. The values are the mean \pm SE of three independent experiments.

apoptosis compared to a 5.0-fold induction caused by C8-ceramide ($p = 0.008$).

Analogue 3 Inhibits Proliferation and Sphingosine-1-phosphate Levels in Chemoresistant Breast Cancer Cells. Both **3** and C8-ceramide have similar survival IC_{50} values in MCF-7 cells, and the disparity in proapoptotic ability led us to evaluate the ability of **3** to block proliferation as an anti-survival mechanism in addition to apoptosis. The capacity of novel drugs to inhibit long-term survival and proliferation is essential in determining the therapeutic potential of any new treatment.^{12,13} We found that **3** has a greater antiproliferative effect than C8-ceramide in MCF-7, MDA-MB-231, and MCF-7TN-R cell lines, with IC_{50} of 4.5, 1.8, and $1.2 \mu\text{M}$, respectively (Figure 3).

Selective toxicity for cancer, but not normal, cells is essential in the development of targeted cancer experimental therapeutics. To determine the selectivity of **3** and C8-ceramide to inhibit cell growth of cancer cells, we performed proliferation assays using MCF10A (normal breast epithelial) cells (Figure 4). Interestingly, **3** and C8-ceramide showed little effect on normal breast epithelial proliferation, even at $100 \mu\text{M}$, which is greater than 50-fold of the IC_{50} in chemoresistant cells.

The increased potency of **3** in hormone therapy resistant and chemoresistant breast cancer cells compared to drug sensitive MCF-7 cells led us to evaluate the effect of this analogue on endogenous sphingolipid levels compared to C8-ceramide (Figure 5). We demonstrate that dihydrospingosine is elevated following **3** treatment, with almost a 50-fold increase in MCF-7TN-R cells. Sphingosine-1-phosphate, the proliferative metabolite of ceramide, decreased in all three cell lines. Interestingly, C8-ceramide had the opposite effect and increased sphingosine-1-phosphate levels. These results correlate with the increased potency of **3** in reducing proliferation in MDA-MB-231 and MCF-7TN-R cells.

Discussion

All six novel ceramide analogues studied were designed to have the same long chain backbone containing 17 carbons and 1 amide nitrogen. This new amide functional group replaced the allyl alcohol functional group of the C8-ceramide. It was previously believed that the enol trans double bond contributes to ceramide's biological activity. However, our results show that **3**, lacking this enol functional group, is an effective

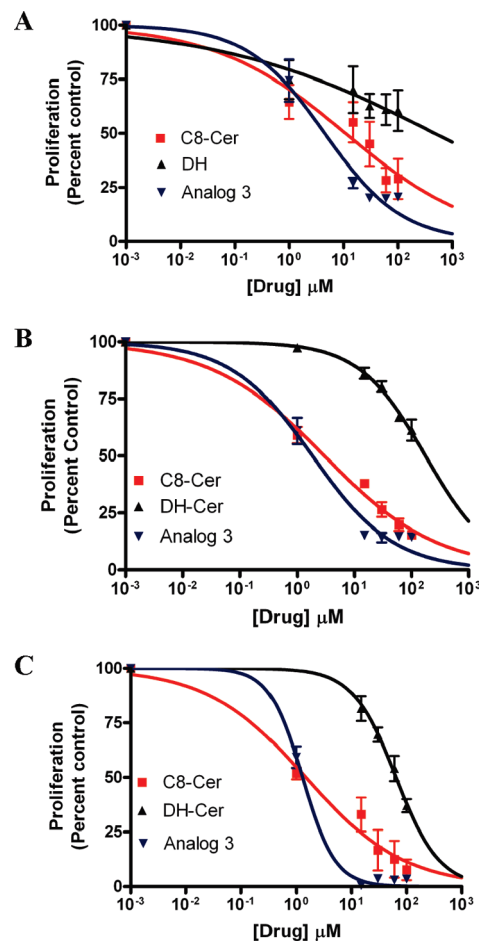


Figure 3. Effect of **3** on breast cancer proliferation. (A) MCF-7, (B) MDA-MB-231, and (C) MCF-7TN-R cells were treated with varying concentrations of ceramide analogue (0.1 – $100 \mu\text{M}$) for 24 h. The values are the mean \pm SE of three independent experiments.

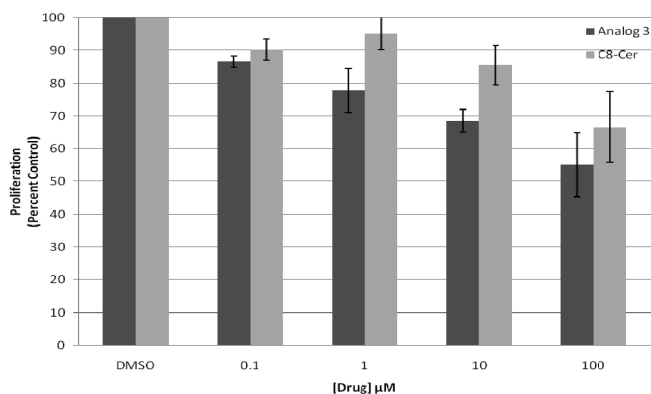


Figure 4. Effect of **3** and C8-ceramide on normal breast proliferation. MCF10A cells were treated with varying concentrations of drug (0.1 – $100 \mu\text{M}$) for 24 h. The values are the mean \pm SE of four independent experiments.

ceramide analogue. The presence of the new amide functional group and the length of the carbon backbone cause a change in polarity and improve the facility of passage through membranes. Other structural variations are the presence and absence of the original amide carbonyl group and different sizes and shapes of the substituents on the original nitrogen. Analogues **1**, **4**, **5**, and **6** contain the original amide group of ceramides but are not potent antisurvival agents. Analogues **2**

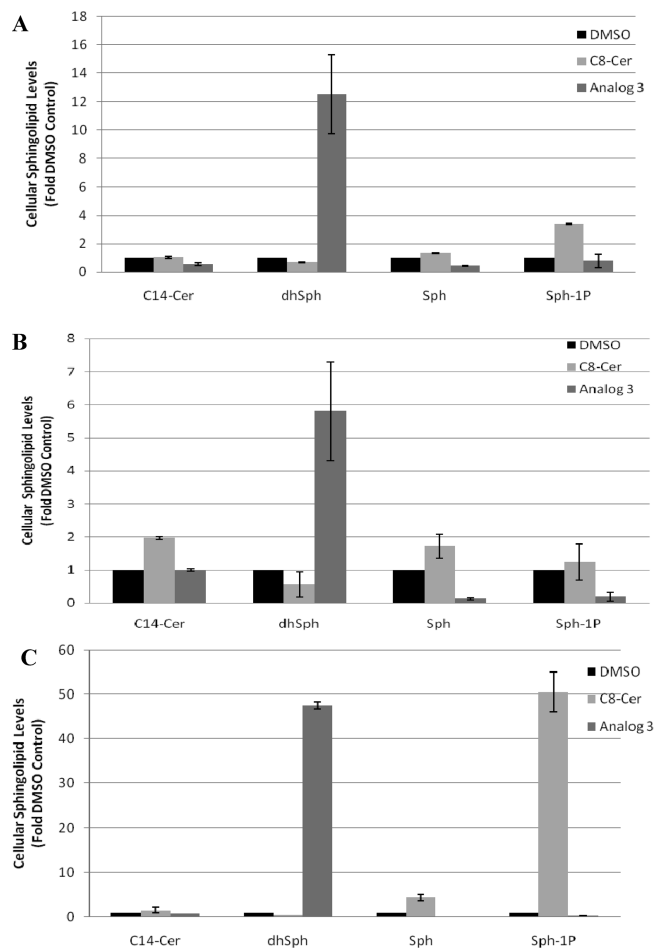


Figure 5. Effect of **3** on cellular sphingolipid species. (A) MCF-7, (B) MDA-MB-231, and (C) MCF-7TN-R cells were treated with ceramide (10 μ M) and **3** (10 μ M) for 24 h. The values are the mean \pm SE of two independent experiments.

and **3**, both lacking the original amide carbonyl group, show the greatest efficacy in MCF-7 cells, endocrine-resistant MDA-MB-231 cells, and chemoresistant MCF-7TN-R cells. This indicates that this modification at the original N atom of ceramide increases the antisurvival effect of the ceramide analogues. Since the main metabolic pathway of ceramide is based on the original amide functional group, the increased antisurvival effect of these ceramide analogues in comparison with ceramide is most probably due to a change in metabolism. Analogues **2** and **3** also share another important structural feature, a benzyl substituent, not present in the other analogues. Their only structural difference is the presence of a carbon–nitrogen double bond in **3** in place of a carbon–nitrogen single bond in **2**. This minor structural difference has led to significant changes in the antiproliferation activity between these analogues. The benzylideneamino group in **3** is harder to hydrolyze than the benzylamino group in **2**. Ceramides cause apoptosis through their interactions with caspases and other apoptotic signaling pathways. Since the hydrolysis of ceramides and ceramide analogues by the enzyme ceramidase leads to sphingosine or sphingosine analogues that are metabolized to form the cell growth-promoting sphingosine-1-phosphate or similar analogues, slower metabolism by hydrolysis is expected to lead to increased ceramide or ceramide analogue concentrations in the cells and higher apoptotic activity.¹⁰ Taken together, our results show that

pharmacological intervention using ceramide-based therapy has therapeutic potential in treating drug resistant breast cancer.

Acknowledgment. We thank Steven Elliott for technical expertise in performing apoptosis assays and Dr. James Robinson's laboratory at Tulane for help in quantifying apoptosis and MTT results. We also thank Dr. Jacek Bielawski and the M.U.S.C. Lipidomics Core for their assistance and expediency in quantifying cellular lipid levels. This research was supported by a grant from the Louisiana Cancer Research Consortium (Grant 631324).

Supporting Information Available: Experimental conditions and analytical data for analogues **1–6**. This material is available free of charge via the Internet at <http://pubs.acs.org>.

References

- (1) Simstein, R.; Burow, M.; Parker, A.; Weldon, C.; Beckman, B. Apoptosis, chemoresistance, and breast cancer: insights from the MCF-7 cell model system. *Exp. Biol. Med. (Maywood, NJ, U. S.)* **2003**, *228*, 995–1003.
- (2) Shabbits, J. A.; Mayer, L. D. P-Glycoprotein modulates ceramide-mediated sensitivity of human breast cancer cells to tubulin-binding anticancer drugs. *Mol. Cancer Ther.* **2002**, *1*, 205–213.
- (3) Gouaze-Andersson, V.; Yu, J. Y.; Kreitenberg, A. J.; Bielawska, A.; Giuliano, A. E.; Cabot, M. C. Ceramide and glucosylceramide upregulate expression of the multidrug resistance gene MDR1 in cancer cells. *Biochim. Biophys. Acta* **2007**, *1771*, 1407–1417.
- (4) Liu, Y. Y.; Yu, J. Y.; Yin, D.; Patwardhan, G. A.; Gupta, V.; Hirabayashi, Y.; Holleran, W. M.; Giuliano, A. E.; Jazwinski, S. M.; Gouaze-Andersson, V.; Consoli, D. P.; Cabot, M. C. A role for ceramide in driving cancer cell resistance to doxorubicin. *FASEB J.* **2008**, *22*, 2541–2551.
- (5) Schiffmann, S.; Sandner, J.; Birod, K.; Wobst, I.; Angioni, C.; Ruckhaberle, E.; Kaufmann, M.; Ackermann, H.; Lotsch, J.; Schmidt, H.; Geisslinger, G.; Grosch, S. Ceramide synthases and ceramide levels are increased in breast cancer tissue. *Carcinogenesis* **2009**, *30*, 745–752.
- (6) Qiu, L.; Zhou, C.; Sun, Y.; Di, W.; Scheffler, E.; Healey, S.; Wanebo, H.; Kouttab, N.; Chu, W.; Wan, Y. Paclitaxel and ceramide synergistically induce cell death with transient activation of EGFR and ERK pathway in pancreatic cancer cells. *Oncol. Rep.* **2006**, *16*, 907–913.
- (7) Lucci, A.; Giuliano, A. E.; Han, T. Y.; Dinur, T.; Liu, Y. Y.; Senchenkov, A.; Cabot, M. C. Ceramide toxicity and metabolism differ in wild-type and multidrug-resistant cancer cells. *Int. J. Oncol.* **1999**, *15*, 535–540.
- (8) Liu, Y. Y.; Han, T. Y.; Giuliano, A. E.; Cabot, M. C. Expression of glucosylceramide synthase, converting ceramide to glucosylceramide, confers adriamycin resistance in human breast cancer cells. *J. Biol. Chem.* **1999**, *274*, 1140–1146.
- (9) Ameyar, M.; Atfi, A.; Cai, Z.; Stancou, R.; Shatrov, V.; Betteieb, A.; Chouaib, S. Analysis of human breast adenocarcinoma MCF7 resistance to tumor necrosis factor-induced cell death. Lack of correlation between JNK activation and ceramide pathway. *J. Biol. Chem.* **1998**, *273*, 29002–29008.
- (10) Struckhoff, A. P.; Bittman, R.; Burow, M. E.; Clejan, S.; Elliott, S.; Hammond, T.; Tang, Y.; Beckman, B. S. Novel ceramide analogs as potential chemotherapeutic agents in breast cancer. *J. Pharmacol. Exp. Ther.* **2004**, *309*, 523–532.
- (11) Weldon, C. B.; Parker, A. P.; Patten, D.; Elliott, S.; Tang, Y.; Frigo, D. E.; Dugan, C. M.; Coakley, E. L.; Butler, N. N.; Clayton, J. L.; Alam, J.; Curiel, T. J.; Beckman, B. S.; Jaffe, B. M.; Burow, M. E. Sensitization of apoptotically-resistant breast carcinoma cells to TNF and TRAIL by inhibition of p38 mitogen-activated protein kinase signaling. *Int. J. Oncol.* **2004**, *24*, 1473–1480.
- (12) Yacoub, A.; Mitchell, C.; Brannon, J.; Rosenberg, E.; Qiao, L.; McKinstry, R.; Linehan, W. M.; Su, Z. S.; Sarkar, D.; Lebedeva, I. V.; Valerie, K.; Gopalkrishnan, R. V.; Grant, S.; Fisher, P. B.; Dent, P. MDA-7 (interleukin-24) inhibits the proliferation of renal carcinoma cells and interacts with free radicals to promote cell death and loss of reproductive capacity. *Mol. Cancer Ther.* **2003**, *2*, 623–632.
- (13) Meeran, S. M.; Katiyar, S.; Elmets, C. A.; Katiyar, S. K. Interleukin-12 deficiency is permissive for angiogenesis in UV radiation-induced skin tumors. *Cancer Res.* **2007**, *67*, 3785–3793.